



Multilayer silver nanoparticles-modified optical fiber tip for high performance SERS remote sensing

Gustavo F.S. Andrade¹, MeiKun Fan¹, Alexandre G. Brolo*

Department of Chemistry, University of Victoria, PO Box 3055, Victoria, BC, Canada V8W 3V6

ARTICLE INFO

Article history:

Received 17 November 2009

Received in revised form 15 February 2010

Accepted 3 March 2010

Available online 10 March 2010

Keywords:

Surface-enhanced Raman scattering (SERS)

Optical fiber

Nanoparticles

Self-assembly

Raman imaging

Remote sensing

ABSTRACT

This work presents the construction and optimization of nanoparticles-modified optical fiber tip (NPs-MOFT) devices for remote sensing by surface-enhanced Raman scattering (SERS). Silver nanoparticles (Ag-NPs) were self-assembled on optical fiber tips through a “layer-by-layer” procedure. It is shown that the SERS performance is at optimum when 5 “layers” of 50 nm Ag-NPs were deposited on the optical fiber tip. Using the optimized Ag-NPs-MOFT device, it was possible to detect 200 nM of the R6G dye in remote sensing mode (backscattering through the fiber). It was also possible to detect dye molecules with different structures and charges at the micro-molar concentration level, including anions, cations and neutral species. It can be envisioned that the Ag-NPs-MOFT device reported in this work can be further developed for SERS-based remote biosensing.

© 2010 Elsevier B.V. All rights reserved.

1. Introduction

The discovery of the surface-enhanced Raman scattering (SERS) effect 35 years ago (Albrecht and Creighton, 1977; Fleischm et al., 1974; Jeanmaire and Vanduyne, 1977) paved the way for the extension of Raman spectroscopy to the realm of trace detection. The use of SERS as an analytical tool has grown over the past years (Bell and Sirimuthu, 2008; Scaffidi et al., 2009; Spuch-Calvar et al., 2009), although there are still a few drawbacks that prevent its widespread application (Bell and Sirimuthu, 2008). The SERS technique proved to be able to detect single molecules (Kneipp et al., 1997; Nie and Emery, 1997). This property qualifies the technique as one of the few that reached this level of sensitivity, in addition to, for instance, fluorescence and scanning-tunnelling microscopy. This positions SERS as one of the few ultimate analytical tools available nowadays. Single-molecule SERS has been reported from different environments (Pieczonka and Aroca, 2008), including under electrochemical conditions (dos Santos et al., 2009), and in single living cells (Scaffidi et al., 2009).

Fiber optics based sensors, on the other hand, have been developed for several spectroscopic techniques, including normal Raman and SERS (Lieberman, 1993; McDonagh et al., 2008). Sensors based on optical fiber are suitable for remote detection and can easily

be implemented to in-field measurements (Stoddart and White, 2009). However, fiber optic sensors based on SERS received much less attention than normal Raman (Stoddart and White, 2009; Vo-Dinh and Stokes, 2002). The several approaches that can be used for engineering optical fibers for SERS can be divided into two main groups: optrodes and cladding-coupled sensors.

The cladding-coupled sensor is based on the evanescent field between the core and the cladding of the optical fiber. The fiber is polished or etched carefully to decrease the cladding thickness allowing higher intensity for the evanescent field. The resulting fiber is then modified on the thin clad area with a silver or a gold layer. The evanescent field is used to excite the SERS (Zhang et al., 2005). This procedure usually leads to very fragile sensors, and the re-coupling of the Raman scattered light is very inefficient, resulting in limited Raman sensitivity.

For the optrode approach, the tip of one (or a bundle) of optical fibers are modified by the SERS-active layer, and the laser collection can be done either in backscattering through the same fiber or by forward scattering using a separated set of fibers. The first reports on optrodes relied on the concept of using a metal-modified optical fiber tip as the SERS substrate, and a collection fiber to couple the SERS signal to the spectrometer (Bello et al., 1990; Mullen and Carron, 1991). Stokes and Vo-Dinh (2000) reported the use of microparticles of alumina covered with Ag, and Polwart et al. (2000) reported the immobilization of Ag nanoparticles on the tip of an optical fiber as single-fibers SERS optrodes. Several authors proposed other procedures to obtain optrodes, including photochemical modification (Zheng et al., 2008), evaporation of

* Corresponding author. Tel.: +1 250 721 7167; fax: +1 250 721 7147.

E-mail address: agbrolo@uvic.ca (A.G. Brolo).

¹ These authors contributed equally to this work.

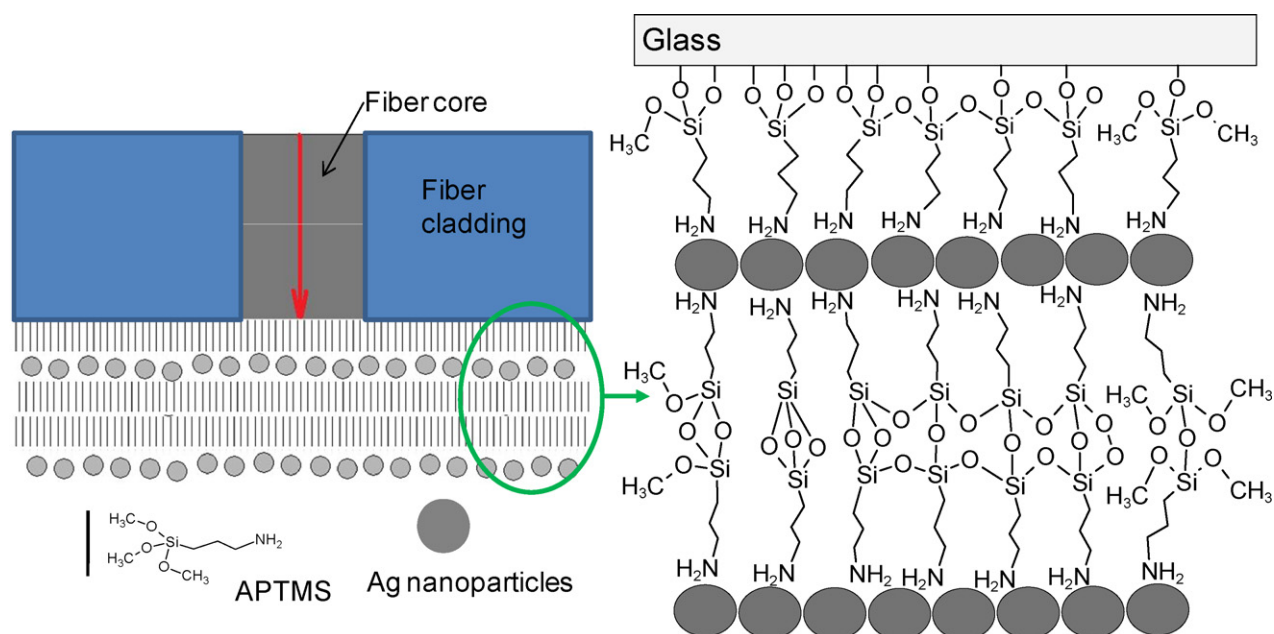


Fig. 1. Configuration of the optical fiber tip modified with "multilayer" of Ag-NPs.

metal films (Hankus et al., 2006; Viets and Hill, 1998), nanoimprint lithography (Kostovski et al., 2009), and electron beam lithography (Smythe et al., 2009). However, some of these sensors showed a limited sensitivity and they were not suitable for carrying both excitation and Raman photons at the same time, which prevented their application in remote sensing.

In our previous works, it was found that the SERS performance of metallic nanoparticles (MNPs) modified substrate is greatly depended on the number of MNPs depositions (Addison and Brolo, 2006; Fan and Brolo, 2009, 2008), because larger deposition number tends to increase the density of NPs on the surface, which in turn yields to a higher population of SERS hot-spots. At optimized MNPs deposition numbers, the SERS signal can be orders of magnitude higher than for just one MNPs deposition, depending on the laser frequency, the solid support and the nature of the MNPs. Furthermore, the sample-to-sample reproducibility was also greatly improved with increasing deposition numbers (Fan and Brolo, 2009, 2008). In the present work, we extend the use of this methodology to modify OFTs with Ag-NPs. We will show that the Ag nanoparticles-modified optical fiber tip (Ag-NPs-MOFT) devices fabricated in this way have very good sensitivity and reproducibility. Most importantly, this device is suitable for remote sensing. As a proof of concept, remote detection of several dyes with diverse chemical structures was performed using the Ag-NPs-MOFT device.

2. Materials and methods

2.1. Chemicals

Unless otherwise mentioned, ACS grade chemicals were used. AgNO_3 , sodium citrate di-hydrate, 3-aminopropyltrimethoxysilane (APTMS) and Nile Blue A (NBA) perchlorate were obtained from Sigma-Aldrich. Rhodamine-6G (R6G), 4-dicyanomethylene-2-methyl-6-(p(dimethylamino)styryl)-4H-pyran (DCM) and Congo Red (CR) were obtained from LambdaChrome. Ultrapure water with a resistivity of $18.2 \text{ M}\Omega \text{ cm}$ (Barnstead NANOpure Diamond water purification system) was used throughout the experiments. Methanol (Calderon, HPLC grade) was used without further purification.

2.2. Ag-NPs synthesis and the immobilization on OFT

The preparation of Ag-NPs follows the procedure reported in the literature (Cui et al., 2006). Briefly, a 500 mL AgNO_3 solution ($5.29 \times 10^{-4} \text{ M}$) was brought to boiling under vigorous stirring. Then, 10 mL of 1% sodium citrate solution was quickly added. The heating and stirring were kept for an hour and then only with stirring until the solution cool to room temperature. The as prepared Ag-NPs showed an absorption peak at $\sim 399 \text{ nm}$.

The APTMS sol-gel was prepared by following a method for 3-mercaptopropyltrimethoxysilane (Fan and Brolo, 2009; Jena and Raj, 2006). Briefly, 400 μL of APTMS and 332 μL of 0.1 M HCl were added into 33 mL of water. The solution was vigorously stirred for at least 1 h. The sol-gel mixture shall be used the same day. The Ag-NPs self-assembly procedure was similar to our previous work of Ag-NPs on glass slide and it is illustrated in Fig. 1 (Fan and Brolo, 2009). The single-mode optical fiber (F-SA from Newport, with 2 μm core diameter) was cut into $\sim 40 \text{ cm}$ long segments.

Before the modification, the polymer protection layer close to the tip of the fiber ($\sim 3 \text{ cm}$) was peeled off, and then the tip was cleaved using a ceramic cutter to obtain a flat surface. The OFT was then cleaned in piranha solution for 20 min and washed thoroughly with deionized water. After drying under N_2 gas flow, it was soaked in a 10 mM APTMS ethanolic solution for 24 h. Following the modification with APTMS, the OFT was thoroughly washed with deionized water, dried and soaked for additional 24 h in the Ag-NPs suspension. Finally, it was washed with deionized water and dried under N_2 again. For the deposition of additional Ag-NPs layers, the OFT was soaked for 20 min in the APTMS sol-gel solution and followed by 1 h in the Ag-NPs suspension, with vigorous rinsing with deionized water between steps. This procedure was repeated until the desired number of "layers" was obtained. After the last desired layer of Ag-NPs was deposited, the Ag-NPs-MOFT was heated up in N_2 atmosphere to $\sim 110^\circ \text{C}$ for 15 min to induce cross linking among the APTMS sol-gel and improve the stability of the modifier layers of Ag-NPs (Polwart et al., 2000).

SEM images were obtained for Ag-NPs-MOFT device after 5 Ag-NPs-depositions, and they are shown as supplementary material (Fig. S1). The SEM images clearly showed that a homogeneous, high density, assembly of Ag-NPs on the fiber tip was achieved,

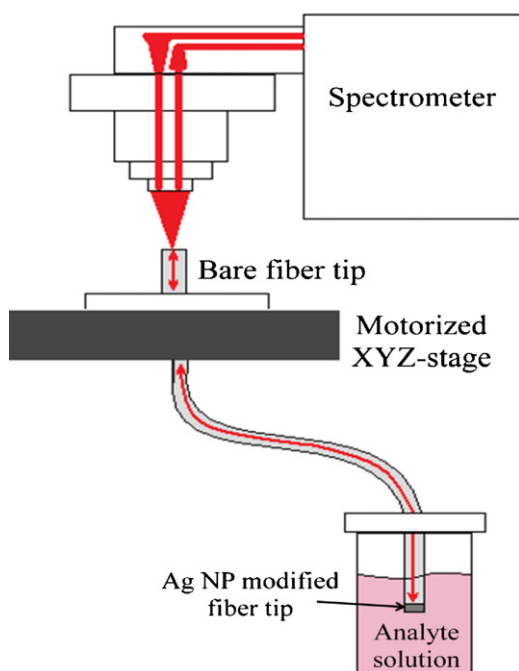


Fig. 2. Scheme for the SERS experiments using the Ag-NP-OFT devices.

as observed before for Ag-NPs depositions on planar glass slides (Fan and Brolo, 2009).

2.3. SERS spectra

The SERS spectra were obtained in a Renishaw InVia Raman spectrometer, equipped with the 632.8 nm line from a He–Ne laser (4.5 mW of power on the objective). The objective used was a 50 \times magnification, with NA (numerical aperture) = 0.75. The full-width at half-maximum (FWHM) of the He–Ne laser spot for this objective is 0.9 μm . The spectrometer is also equipped with a motorized stage that allows the computer-controlled XYZ positioning of the sample, which was used to obtain the Raman mappings.

The SERS spectra were obtained sending the laser light through the 50 \times objective to the unmodified proximal tip of the optical fiber, with the distal Ag-NPs-modified tip immersed in the analyte aqueous solution, as shown in Fig. 2. The SERS mapping was obtained by moving the motorized stage of the Renishaw InVia microscope in both X and Y directions at step size of 0.5 μm . A SERS spectrum was recorded in each spot from the proximal fiber tip (unmodified tip). To obtain the SERS map, the peak area of the strongest SERS band (1508 cm^{-1}) of R6G was plotted as a function of the X–Y position. The SERS intensity is color-coded; the brighter colors represent higher intensities. It should be noticed that methanolic solutions were also used, but the SERS performance of the Ag-NP-OFT was lower in this solvent. Both excitation and collection were in the proximal tip of the modified fiber, which is the configuration suitable for remote sensing (Fan and Brolo, 2009).

3. Results and discussion

The optical fibers used in the work were single mode in the visible light range, and the diameter of their core was 2 μm . The diameter of the core used in this work is smaller than that in previous works (Stoddart and White, 2009), which is justified by the fact that it is a single-mode optical fiber in the 632.8 nm region. This will minimize light loss during the SERS measurements. The small core caused the coupling of light possible only in a small area of the fiber tip. In order to get the best possible coupling, the fiber holder was

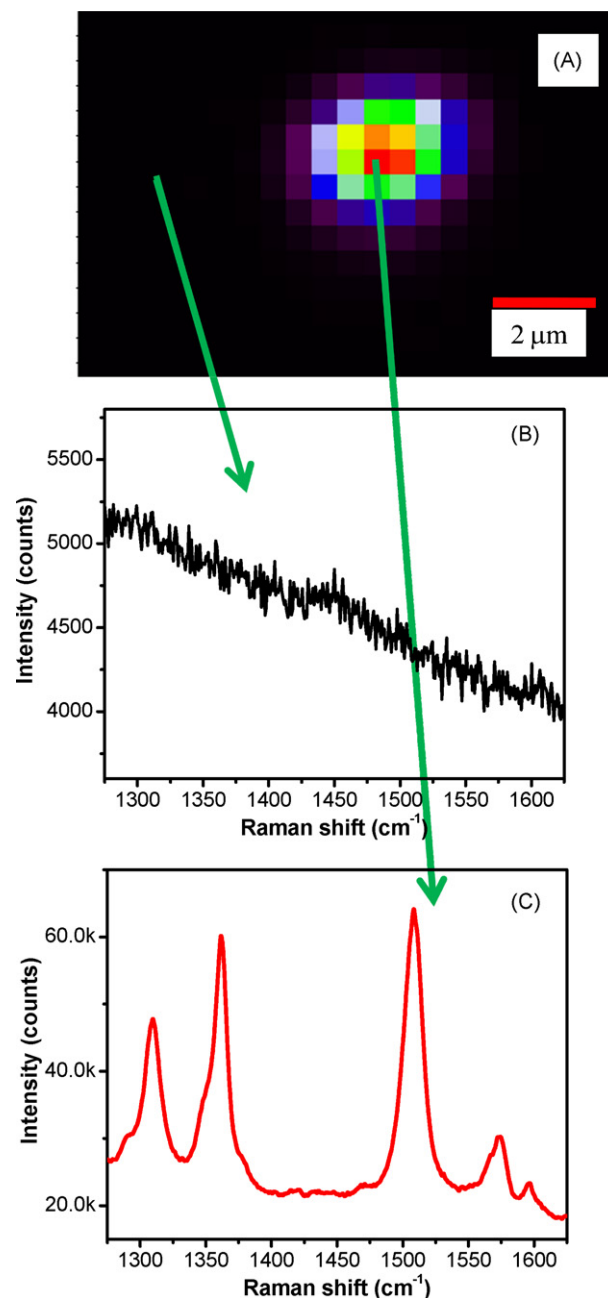


Fig. 3. (A) Raman mapping for the 1508 cm^{-1} band of R6G on a 5 layers Ag-NPs-MOFT. (B) and (C) Raman spectra corresponding to the points of the Raman mapping indicated by the green arrows from (A).

mounted on the motorized stage in the Raman microspectrometer as shown in Fig. 2.

The Raman spectra were acquired sending the laser light from the proximal unmodified tip throughout the whole fiber length, and collecting the light backscattered from the distal modified fiber tip, as depicted in Fig. 2. The setup shown in Fig. 2 is intended to allow the use of the device for remote sensing, because the modified tip can be directly introduced into the sampling environment. In the present work, the samples were in vials away from the spectrometer, the Ag-NPs-modified optical fiber tip was simply immersed in the sample solution without any special mount.

A Raman mapping at the unmodified tip was performed to find an optimum spot that presents the maximum SERS signal, which is expected to be at the center of the fiber core. In this kind of measurement, the computer-controlled motorized XYZ-stage stop in

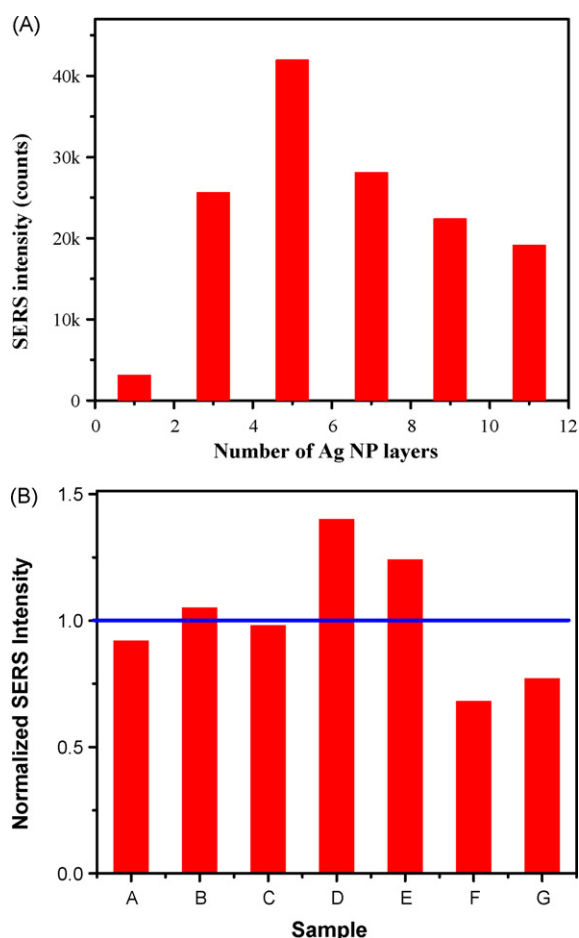


Fig. 4. (A) SERS performance of the NPs–MOFT as a function of the number of Ag–NPs deposited (only the odd deposition numbers are shown). (B) Average normalized SERS intensity distribution of the 1508 cm^{-1} band intensity for 7 different 5 Ag–NPs monolayer samples.

one spot and one Raman spectrum is taken; following this, the XYZ-stage moves to the next spot and a new spectrum is obtained. This process is repeated in a pre-determined area of the sample. After the completion, the intensity of a certain band can be plotted as a function of the position on the sample, generating a 2D-plot. The Raman intensity is color-coded; the brighter colors representing higher intensities.

Fig. 3 shows the Raman mapping for the 1508 cm^{-1} -region of the proximal unmodified tip for a Ag–NPs–MOFT immersed in a $10\text{ }\mu\text{M}$ R6G dye solution. The Raman mapping in Fig. 3A shows that no SERS from R6G can be detected in most of the area of the fiber tip (Fig. 3B), but only from a small spot, which corresponds to the fiber core, the R6G SERS spectra with a high signal-to-noise ratio can be observed (Fig. 3C). The SERS performance evaluation of the device was based on the most intense spectra from the Raman mappings, which corresponds to the middle of the fiber core, where most of the light is coupled.

The “layer-by-layer” procedure allows multiple depositions of Ag–NPs on glass using the APTMS sol–gel as linker (Fan and Brolo, 2009). Fig. 4A presents the SERS intensity of the 1508 cm^{-1} band of $10\text{ }\mu\text{M}$ R6G on the NPs–MOFT devices as a function of the number of Ag–NPs layers deposited.

It can be noticed in Fig. 4A that the SERS intensity is maximized after 5 Ag–NPs depositions. The maximum SERS intensity was roughly 10 times higher than for just one deposition. Further increase in the number of Ag–NPs deposition decreased the SERS signal. Fan and Brolo (2009) studied the SERS intensity dependence

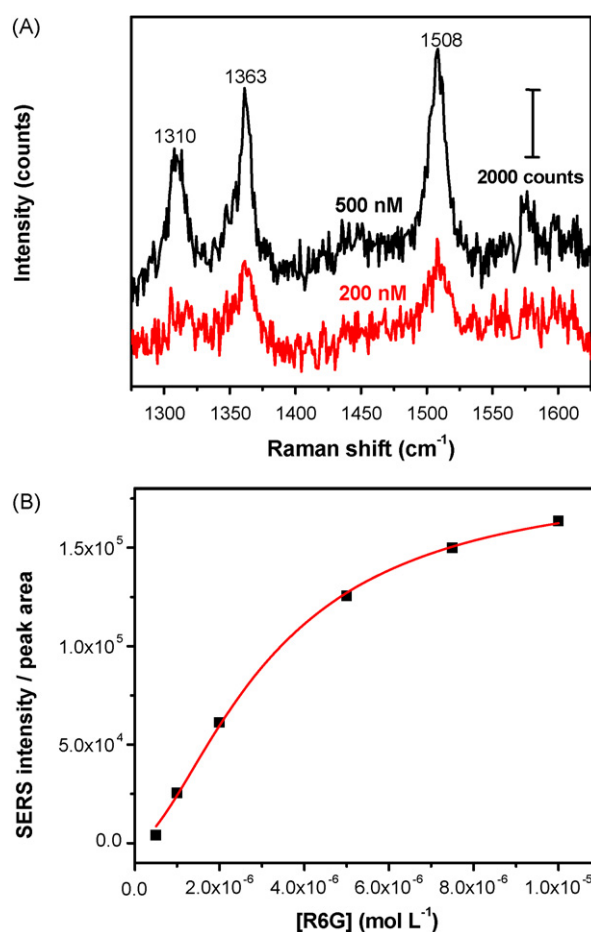


Fig. 5. (A) SERS of R6G at different concentrations obtained from a 5 deposition made Ag–NPs–MOFT. The baseline was subtracted and the spectra were offset for clarity; (B) (black squares) a signal–dose curve for R6G in water using the band (peak area) at 1508 cm^{-1} ; (red line) fitting of a Langmuir–Freundlich isotherm curve to the experimental points, used to obtain the LOD for the Ag–NPs–MOFT device. (For interpretation of the references to color in this figure legend, the reader is referred to the web version of the article.)

with the number of Ag–NPs deposition on glass slides and found that the maximum intensity was from 6 layers of Ag–NPs. Also, further increase in the number of Ag–NPs deposition on glass slides did not affect the SERS intensity after the maximum. The decrease in SERS signal after 5 Ag–NPs deposition, shown in Fig. 4A, can be rationalized by taking into account the SERS measurement configuration. The laser excitation must travel through the fiber, excite the Ag–NPs at the tip from the glass side and interact with molecules adsorbed at the Ag NPs – solution interface. The scattered light must couple back into the fiber to reach the spectrometer. Therefore, it must be a balance between the thickness of the metal layer and the arrangement of the nanostructures to generate the required hot-spots for SERS. The increase in SERS intensity from 1 to 5 depositions might be assigned to an increase in the number of hot-spots accessible to the adsorbed species. After 5 Ag–NPs deposition, the thickness of the metal layer become significantly large, decreasing the efficiency of both excitation and collection through the metal film.

One of the major concerns on the development of SERS substrates is the sample-to-sample reproducibility of the SERS signal. Fig. 4B presents the SERS intensity from R6G $10\text{ }\mu\text{M}$ solution for seven samples of the optimized 5 layers Ag–NPs–MOFT device. The relative standard deviation (RSD%) for this device was around 25%, which is consistent with previous reports (Fan and Brolo, 2009, 2008).

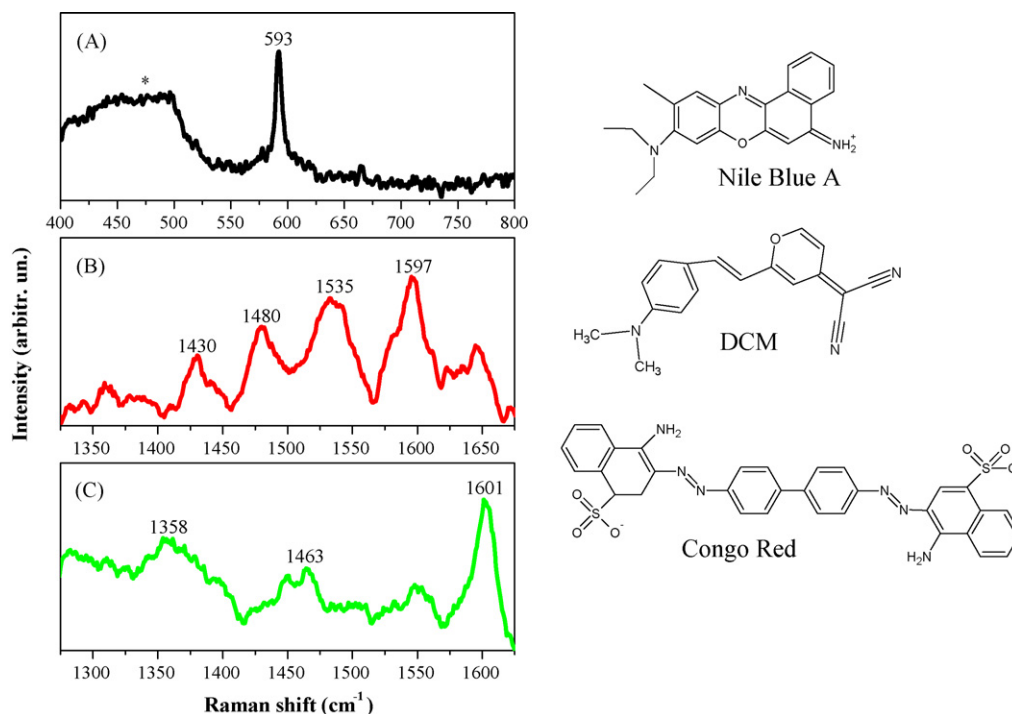


Fig. 6. SERS spectra of 1.0 μM aqueous solutions of the dyes: (A) Nile Blue A; (B) DCM; (C) Congo Red. The chemical structure of the dyes is shown on the right of the SERS spectra.

The minimum amount of analyte that can be detected by the Ag-NPs-MOFT was also explored. Fig. 5A presents SERS spectra from 200 and 500 nM R6G solutions obtained using an optimized Ag-NPs-MOFT device. It is worth mentioning that the two measurements were made with the same Ag-NPs-MOFT, starting from the lowest concentration and with a washing step between measurements. One can notice in Fig. 5A that it is possible to observe the characteristic SERS bands of R6G for concentration as low as 200 nM. In previous reports on metal-modified single optical fiber tips for backscattering detection using SERS, Polwart et al. (2000) detected crystal violet down to 100 nM and Lan et al. (2009) reported optodes that could detect R6G down to 10 nM with the addition of NaCl to the solution containing the dye. Shi et al. (2008) reported the detection of R6G in concentrations as low as 1 nM with the addition of Ag-NPs to the analyte solution, and Kostovski et al. (2009) reported the detection of one monolayer of thiophenol and 100 μM of R6G. In Fig. 5B, a calibration curve for one of our Ag-NPs-MOFT is shown. The SERS intensity (in peak area) versus the concentration of R6G was well fitted using a Langmuir–Freundlich isotherm ($R^2 = 0.998$), and the limit-of-detection (LOD) was determined to be 3 nM for the Ag-NP-MOFT device in remote sensing mode. To our knowledge, this report is probably one of the lowest concentrations achieved using the real time remote sensing configuration, and without the help of any extra reagents other than the analyte. The equilibrium constant for R6G adsorption on Ag-NPs and the saturation coverage were also obtained from the isotherm, and they are in good agreement with a previous work (Hildebrandt and Stockburger, 1984), as discussed in more details in the Supporting Information.

Hence, this high sensitivity property, in addition to the ease fabrication and high reproducibility, shows a considerable promise for this SERS device in remote sensing.

It is also worth mentioning that the sensor area that actually contributes to the SERS signal contains hot-spots within the ca. 3 μm^2 fiber core. The surface coverage of R6G is expected to be low at these concentrations (dos Santos et al., 2009; Hildebrandt and

Stockburger, 1984), the combination of low surface coverage and small number of hot-spots limits the probability of R6G molecules to populate the sites that contribute mostly to the signal (hot-spots) (dos Santos et al., 2009). The detection of R6G for concentrations lower than 200 nM, as observed in our previous report for Ag-NPs adsorbed on glass slides (Fan and Brolo, 2009), could be achievable, but it would probably require a long immersion time to collect the sample due to the even lower probability of R6G molecules to find a hot-spot.

The stability of the Ag-NPs-MOFT device was also examined. It was found that there is no loss of SERS activity for the device when stored in air for 72 h. However, the SERS performance of the device decreased dramatically after storage in water for 24 h, and it was completely lost after storage in methanolic solution for the same period of time. The decrease in SERS intensity might be related to the solvolysis of the silane linker layer (Plueddemann, 1991). This limitation affects prolonged measurements using a single Ag-NPs-MOFT device, especially in methanolic environment. These limitations are offset by some of the advantages of the device; including easy fabrication involving standard chemicals and well-established wet chemistry methods that can be easily extended to mass production, and, most importantly, the reasonable sample-to-sample reproducibility (RSD% of $\sim 25\%$).

Metallic NPs made from different methods usually are known to have different surface charges, and hence favour the adsorption of certain types of analytes, which strongly correlates with the average SERS intensity (Alvarez-Puebla and Aroca, 2009). Hence, the ability to detect molecules with very different structures and charges without pre-treatment of sample is an extremely desirable property for SERS remote sensors. This kind of property could make the sensor useful for cellular studies in the future, where labeling with multiple organic dyes are common practice (Hanson and Hanson, 2008). The Ag-NPs-MOFT device was then tested using a large range of analytes. Fig. 6 presents the SERS spectra of NBA, DCM and CR in concentration of 1 μM on NPs-MOFT devices. These dyes were chosen because they have different charges, as can be

noticed by the chemical structure in the right-hand side of Fig. 6. NBA is a cation, DCM is neutral and CR is an anion and they would have very different affinities for the Ag-NPs surface.

The SERS spectra shown in Fig. 6 confirm that the NPs-MOFT device is able to detect molecules with very different chemical structures at a concentration as low as 1 μM , also without the needs of additional reagents, but with comparable sensitivities to literature reports (Polwart et al., 2000). In the NBA case, the He–Ne laser line is inside the absorption band of the analyte, and presents an additional enhancement due to resonance Raman, characteristics of the surface-enhanced resonance Raman scattering (SERRS) effect. Due to this additional enhancement, the SERS intensity for the 1 μM NBA solution is higher than for the other dyes. It is also worth noticing that the well known silica interference, with a maximum at 460 cm^{-1} (marked with an asterisk in Fig. 6A) is much weaker than the NBA band at 593 cm^{-1} .

4. Conclusions

This work presented the construction and optimization of the NPs-MOFT device for SERS detection of several analytes. The optimization procedure showed that the highest SERS intensity can be obtained after 5 depositions of 50 nm Ag-NPs by a sol–gel procedure on the tip of the optical fiber. Using the optimized 5-layer Ag-NPs-modified device it was possible to detect 200 nM of the R6G dye, and it is also possible to detect molecules with different net charges at the micro-molar concentration limit, including anions, cations and neutral molecules.

The results showed a flexible remote SERS sensor with a very high sensitivity. Although there is some issue with the long time stability when expose to solvents, this problem does not hinder the usage of the device when stored in air. The Ag-NPs-MOFT device can be used as a single-use remote sensing element, since it is easy to fabricate and provide good sample-to-sample reproducibility. It can be envisioned that this kind of device could also be used as a SERS-based biosensor.

Acknowledgment

This work was supported by operating grants from NSERC and by the NSERC Strategic Network for Bioplasmonic Systems (Biop-Sys), Canada. The equipment grant was provided by the Canada Foundation for Innovation (CFI), the British Columbia Knowledge and Development Fund (BCKDF) and the University of Victoria through the New Opportunities Program. G.F.S.A. thanks Canadian Bureau for International Education - Department of Foreign Affairs and International Trade (CBIE-DFAIT) of Canada for a post-doctoral

fellowship. The authors also thank Mohammad M. Rahman for acquiring the SEM images.

Appendix A. Supplementary data

Supplementary data associated with this article can be found, in the online version, at doi:10.1016/j.bios.2010.03.007.

References

- Addison, C.J., Brolo, A.G., 2006. *Langmuir* 22 (21), 8696–8702.
- Albrecht, M.G., Creighton, J.A., 1977. *J. Am. Chem. Soc.* 99 (15), 5215–5217.
- Alvarez-Puebla, R.A., Aroca, R.F., 2009. *Anal. Chem.* 81 (6), 2280–2285.
- Bell, S.E.J., Sirimuthu, N.M.S., 2008. *Chem. Soc. Rev.* 37 (5), 1012–1024.
- Bello, J.M., Narayanan, V.A., Stokes, D.L., Vodinh, T., 1990. *Anal. Chem.* 62 (22), 2437–2441.
- Cui, Y., Ren, B., Yao, J.L., Gu, R.A., Tian, Z.Q., 2006. *J. Phys. Chem. B* 110 (9), 4002–4006.
- dos Santos, D.P., Andrade, G.F.S., Temperini, M.L.A., Brolo, A.G., 2009. *J. Phys. Chem. C* 113 (41), 17737–17744.
- Fan, M., Brolo, A.G., 2009. *Phys. Chem. Chem. Phys.* 11 (34), 7381–7389.
- Fan, M.K., Brolo, A.G., 2008. *ChemPhysChem* 9 (13), 1899–1907.
- Fleischm, M., Hendra, P.J., McQuilla, A.J., 1974. *Chem. Phys. Lett.* 26 (2), 163–166.
- Hankus, M.E., Li, H.G., Gibson, G.J., Cullum, B.M., 2006. *Anal. Chem.* 78 (21), 7535–7546.
- Hanson, G.T., Hanson, B.J., 2008. *Comb. Chem. High Throughput Screening* 11 (7), 505–513.
- Hildebrandt, P., Stockburger, M., 1984. *J. Phys. Chem.* 88 (24), 5935–5944.
- Jeanmaire, D.L., Vanduyne, R.P., 1977. *J. Electroanal. Chem.* 84 (1), 1–20.
- Jena, B.K., Raj, C.R., 2006. *Anal. Chem.* 78 (18), 6332–6339.
- Kneipp, K., Wang, Y., Kneipp, H., Perelman, L.T., Itzkan, I., Dasari, R., Feld, M.S., 1997. *Phys. Rev. Lett.* 78 (9), 1667–1670.
- Kostovski, G., White, D.J., Mitchell, A., Austin, M.W., Stoddart, P.R., 2009. *Biosens. Bioelectron.* 24 (5), 1531–1535.
- Lan, X.W., Han, Y.K., Wei, T., Zhang, Y.N., Jiang, L., Tsai, H.L., Xiao, H., 2009. *Opt. Lett.* 34 (15), 2285–2287.
- Lieberman, R.A., 1993. *Sens. Actuators B: Chem.* 11, 43–55.
- McDonagh, C., Burke, C.S., MacCraith, B.D., 2008. *Chem. Rev.* 108 (2), 400–422.
- Mullen, K.I., Carron, K.T., 1991. *Anal. Chem.* 63 (19), 2196–2199.
- Nie, S.M., Emery, S.R., 1997. *Science* 275 (5303), 1102–1106.
- Pieczonka, N.P.W., Aroca, R.F., 2008. *Chem. Soc. Rev.* 37 (5), 946–954.
- Plueddemann, E.P., 1991. *Silane Coupling Agents*, 2nd ed. Plenum Press, New York.
- Polwart, E., Keir, R.L., Davidson, C.M., Smith, W.E., Sadler, D.A., 2000. *Appl. Spectrosc.* 54 (4), 522–527.
- Scaffidi, J.P., Gregas, M.K., Seewaldt, V., Vo-Dinh, T., 2009. *Anal. Bioanal. Chem.* 393 (4), 1135–1141.
- Shi, C., Yan, H., Gu, C., Ghosh, D., Seballos, L., Chen, S.W., Zhang, J.Z., Chen, B., 2008. *Appl. Phys. Lett.* 92 (10).
- Smythe, E.J., Dickey, M.D., Bao, J.M., Whitesides, G.M., Capasso, F., 2009. *Nano Lett.* 9 (3), 1132–1138.
- Spuch-Calvar, M., Rodriguez-Lorenzo, L., Morales, M.P., Alvarez-Puebla, R.A., Liz-Marzan, L.M., 2009. *J. Phys. Chem. C* 113 (9), 3373–3377.
- Stoddart, P.R., White, D.J., 2009. *Anal. Bioanal. Chem.* 394 (7), 1761–1774.
- Stokes, D.L., Vo-Dinh, T., 2000. *Sens. Actuators B: Chem.* 69 (1–2), 28–36.
- Viets, C., Hill, W., 1998. *Sens. Actuators B: Chem.* 51, 92–99.
- Vo-Dinh, T., Stokes, D.L., 2002. In: Chalmers, J.M., Griffiths, P.R. (Eds.), *Handbook of Vibrational Spectroscopy*. John Wiley & Sons, Chichester, pp. 1302–1317.
- Zhang, Y., Gu, C., Schwartzberg, A.M., Zhang, J.Z., 2005. *Appl. Phys. Lett.* 87 (12).
- Zheng, X.L., Guo, D.W., Shao, Y.L., Jia, S.J., Xu, S.P., Zhao, B., Xu, W.Q., Corredor, C., Lombardi, J.R., 2008. *Langmuir* 24 (8), 4394–4398.